# Factors Influencing the Specificity of Inhibitor Binding to the Human and Malaria Parasite Dihydroorotate Dehydrogenases

Paul T. P. Bedingfield,[†] Deborah Cowen,[‡] Paul Acklam,[§] Fraser Cunningham,[‡] Mark R. Parsons,[†,§] Glenn A. McConkey,*[,†,§] Colin W. G. Fishwick,*[,‡,§] and A. Peter Johnson*[,‡,§]

[†]Faculty of Biological Sciences, [‡]School of Chemistry, and [§]Astbury Centre for Structural Molecular Biology, University of Leeds, Leeds, LS2 9JT, U.K.

S *Supporting Information*

ABSTRACT: The de novo pyrimidine biosynthesis enzyme dihydroorotate dehydrogenase is an emerging drug target for the treatment of malaria. In this context a key property of *Plasmodium falciparum* DHODH (*Pf*DHODH) is that it can be selectively inhibited over its human homologue (*Hs*DHODH). However, *Hs*DHODH is also a validated drug target for autoimmune diseases such as arthritis. Here a series of novel inhibitors is described that includes compounds that switch specificity between the two enzymes as a result of small alterations in chemical structure. Structure−activity relationship (SAR), crystallography, docking, and mutagenesis studies are used to examine the binding modes of the compounds within the two enzymes and to reveal structural changes induced by inhibitor binding. Within this series, compounds with therapeutically relevant *Hs*DHODH activity are described and their binding modes characterized using X-ray crystallography, which reveals a novel conformational shift within the inhibitor binding site.
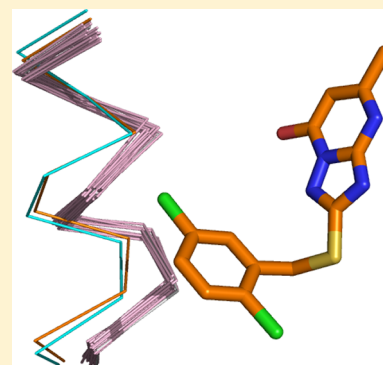
INTRODUCTION

De novo pyrimidine biosynthesis has become a well-established pathway for chemotherapeutic intervention in both humans and the malarial protozoan parasite *Plasmodium falciparum*.[1−9] Pyrimidines are important components in the synthesis of DNA, RNA, glycoprotein, and membrane lipids, all of which are vital for the growth and maintenance of cells.

Malaria is a disease that causes the death of over a million people every year, and *P. falciparum* is responsible for the majority of these fatalities.[10] *P. falciparum* cannot salvage pyrimidines and therefore relies entirely on a de novo biosynthesis pathway. For this reason, the inhibition of the fourth enzyme in the biosynthetic pathway, dihydroorotate dehydrogenase (*Pf*DHODH), is detrimental to the parasite in both cell culture and animal models.[1,11,12]

Unlike *P. falciparum,* humans can salvage preformed pyrimidines as well as synthesize them de novo. Therefore, inhibition of human dihydroorotate dehydrogenase (*Hs*DHODH) is not lethal, but merely slows acquisition of pyrimidines, giving rise to a number of therapeutic responses. Indeed, *Hs*DHODH inhibitors are currently used in the treatment of rheumatoid arthritis[2] and are being evaluated as potential therapeutics for multiple sclerosis,[3] cancer,[4] and even viral infections.[5,6]

However, *Hs*DHODH inhibition also has an immunosuppressive effect that, in most cases, is undesirable in a malarial patient. It is therefore important to be able to develop inhibitors that are selective for *Pf*DHODH over *Hs*DHODH. In earlier studies, chemical derivatives were generated that reversed the selectivity of a potent *Hs*DHODH inhibitor,

resulting in molecules that also inhibited *Pf*DHODH.[13] Further understanding of the structural features within these two enzymes that govern binding selectivity would provide valuable information for the design of selective *Pf*DHODH inhibitors.[7,14,15]

Here, we describe how the application of small molecule inhibitor libraries coupled with crystallographic and mutagenesis studies has provided new insights into the subtle structural differences that appear to be important factors in governing the selectivity of inhibitor binding.

RESULTS

Ligand Based Screening and Chemistry. In order to begin our studies, we wished to create small, focused molecular libraries targeted at both of the DHODH enzymes of interest. Recently, compound **1** (DSM1) (Figure 1) was reported to be a selective inhibitor of *Pf*DHODH by Phillips et al.[16−18] We therefore used this compound as a template for in silico structural similarity searches of databases of commercially available compounds to identify novel chemical scaffolds that might offer potential as DHODH inhibitors. This was achieved using structure **1** as input for the ROCS (rapid overlay of chemical structures) application,[19] which is a tool that can be used to screen for similar molecules to the input template based upon shape, size, and charge profiles. A ROCS screening, using the shape/color combination scoring function, was performed on the Maybridge chemical screening library which had been
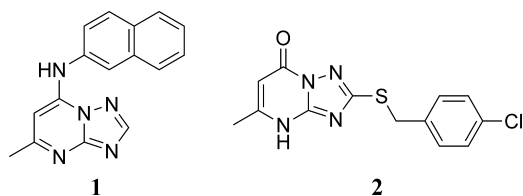
Figure 1. Structures of *Pf*DHODH inhibitors **1** and **2**. Compound **2** is the most active inhibitor against *Pf*DHODH and *Hs*DHODH identified following the ROCS-based screen of the Maybridge chemical screening library. Note that for convenience, **2** is represented as the pyrimidone tautomer, and similarly, other variants of these structures are also represented in the pyrimidone form.

filtered for leadlike compounds and prepared using the default settings within OMEGA,[20] resulting in a library containing approximately 30 000 molecules. From the top-ranked 500 compounds (the ROCS software default) showing acceptable similarity to the search template **1** (the ROCS default of score of >−1.000000 was used) 10 compounds were selected "by eye" on the basis that they displayed a good range of structural diversity while remaining synthetically accessible and were likely to show acceptable aqueous solubility. These compounds were purchased and tested for activity against *Pf*DHODH and *Hs*DHODH, respectively, resulting in compound **2** being identified as the most active against both enzymes (Table 1).

In order to probe the role of structural variation of compound **2** on the inhibitory activity against both enzymes, a series of derivatives were synthesized and tested against both enzymes (Table 1). In particular, compounds **3**−**9** were synthesized in order to assess the significance of position, size, and polarity of the substituent on the aromatic ring within the benzyl portion of the molecule.

Interestingly, the effects of these changes were completely different for the two enzymes. For *Pf*DHODH it was found that varying the position of the chlorine atom from the 4-position, as present in compound **2**, results in reduced inhibition in the order 4-chlorophenyl > 3-chlorophenyl > 2-chlorophenyl. For *Hs*DHODH the opposite trend is observed. Additionally, for all chloro-substituted systems, replacing the

chlorine atom with an alternative substituent does not improve activity and in many cases results in decreased inhibitory activity toward both enzymes. Only the 4-bromo and 2-nitro containing compounds (inhibitors **6** and **8**, respectively) displayed comparable inhibition to their chlorine-based analogue against *Hs*DHODH. The remaining non-chloro-based compounds **5**, **7**, and **9** show reduced inhibitory activity toward both enzymes compared to the corresponding chlorinated systems.

The result of additional substitution within the benzyl portion of compound **2** was explored via the synthesis of compounds **10**−**13**, which all contain a disubstituted benzyl moiety. Compounds **10**, **11**, and **13** were found to display modest activities against both enzymes with the 3,4-dichlorphenyl-containing compound **10** being the most active disubstituted derivative against *Pf*DHODH. Interestingly, the additional chlorine substituent within compound **10** compared to compound **2** does not result in increased potency.

There is, however, a dramatic increase in the *Hs*DHODH inhibitory activity displayed by compound **12** compared to that measured for compounds **10**, **11**, and **13**. This compound has chlorine atoms in the 2 and 5 positions of the benzyl moiety and shows an inhibitory activity of IC$_{50}$ = 51 nM, more than 10000-fold higher than its monochlorinated analogues **3** and **4**.

The activity of compound **12** is on a par with that reported for other very potent *Hs*DHODH inhibitors,[21] and it was therefore decided to explore the detailed binding mode of this compound to *Hs*DHODH using X-ray crystallography. The X-ray cocrystal structure of *Hs*DHODH containing molecule **12** (discussed in detail below) reveals that the inhibitor fills most of the available space within the binding site except for a small pocket near the methyl substituent on the triazolopyrimidine ring (R$_3$, Figure 2).
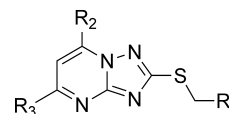

Figure 2. General structure of the *S*-benzyltriazolopyrimidine compounds in Table 1.

Table 1. IC$_{50}$ Values for the *S*-Benzyltriazolopyrimidine Inhibitors against *Pf*DHODH and *Hs*DHODH

compd	R$_1$	R$_2$	R$_3$	IC$_{50}$ ± SE (μM)	
				*Pf*DHODH	*Hs*DHODH
2	4-cholorophenyl	OH	Me	1.0 ± 0.1	39 ± 2
3	2-chlorophenyl	OH	Me	28 ± 4	12 ± 2
4	3-chlorophenyl	OH	Me	5.6 ± 0.3	29 ± 1
5	4-methylphenyl	OH	Me	26 ± 4	46 ± 7
6	4-bromophenyl	OH	Me	33 ± 6	32 ± 6
7	4-methoxyphenyl	OH	Me	21 ± 1	63 ± 31
8	2-nitrophenyl	OH	Me	>100	9.5 ± 7.3
9	phenyl	OH	Me	62 ± 1	89 ± 13
10	3,4-dichlorophenyl	OH	Me	1.9 ± 0.4	6.5 ± 2.7
11	2,6-dichlorophenyl	OH	Me	3.5 ± 1.4	18 ± 3
12	2,5-dichlorophenyl	OH	Me	11 ± 1	0.051 ± 0.007
13	3,5-dimethylphenyl	OH	Me	19 ± 4	30 ± 5
14	4-chlorophenyl	OH	Et	>100	13 ± 1
15	2,5-dichlorophenyl	OH	Et	>100	0.013 ± 0.002
16	phenyl	NH$_2$	Me	>100	>100
17	3,4-dichlorophenyl	NH$_2$	Me	>100	>100
18	phenyl	NHCH$_2$Ph	Me	>100	>100

To further explore the result of varying the substituents at this position, compounds **14** and **15** were synthesized, both of which contain a larger ethyl group in place of the methyl within compound **11**. The inhibitory activities of both of these compounds toward *Hs*DHODH was similar to that found for the methyl-based equivalents, but a distinct loss in inhibitory activity was observed for these compounds toward *Pf*DHODH, suggesting a subtle difference in this region of the protein binding site or a different inhibitor binding mode between the two enzymes.

Compounds **16−18** were synthesized in order to assess the significance of the presence of an oxygen atom at the position R_2 within the inhibitor series. Inclusion of both small (compounds **16** and **17**) and large (compound **18**) amino-based groups at this position resulted in a complete loss in inhibition of both enzymes, emphasizing the importance for binding of the presence of a hydrogen bond acceptor atom at this position and suggesting that these compounds have a binding mode distinct from that reported for molecule **1** in *Pf*DHODH.

Synthesis. Compounds **3−15** were synthesized using a two-step synthesis as detailed in Scheme 1. The reaction times

Scheme 1. Synthesis of Compounds 3−15[a]
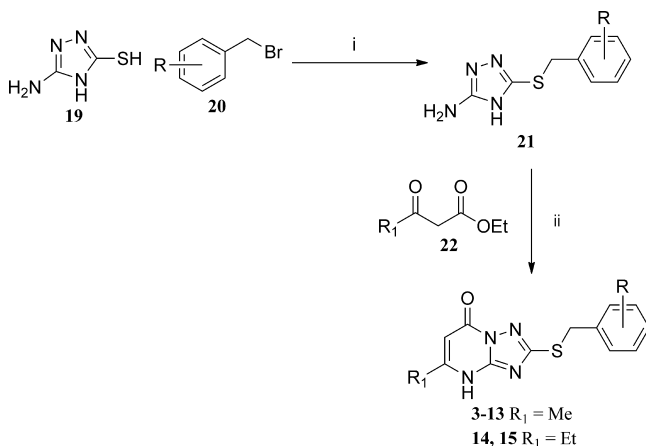
[a](i) K₂CO₃ (1.5 equiv), acetone, 60 °C, 3−9 h, 60−80%; (ii) AcOH, 120 °C, 2−15 h, 50−80%.

varied depending on the substrate, but in general they were short and purification of the products was straightforward. Thiol **19** was selectively alkylated on sulfur to give substituted triazole intermediates **21** in yields ranging from 60% to 80%, followed by cyclization with ethyl acetoacetate **22** (R_1 = Me) or ethyl 3-oxovalerate **22** (R_1 = Et) to produce the target compounds in good yields.

Compounds **16−18** were synthesized using the route shown below (Scheme 2). Treatment of chlorides **24** (obtained from the corresponding alcohols and used without purification) with the appropriate amine yielded compounds **18**, **25**, and **26**, respectively, in high yields (75−95%). Initially, synthesis of intermediate **24** was attempted via treatment of alcohol **9** or **10** with POCl₃ which was unsuccessful, despite literature reports concerning the successful application of this route to this type of chloride;[22−24] however, use of the higher boiling phenyl-phosphonic dichloride for the chlorination proved to be satisfactory. Subsequently compounds **16** and **17** were obtained via deprotection of **25** and **26**, respectively (Scheme 2).

Scheme 2. Synthesis of Compounds 16−18[a]
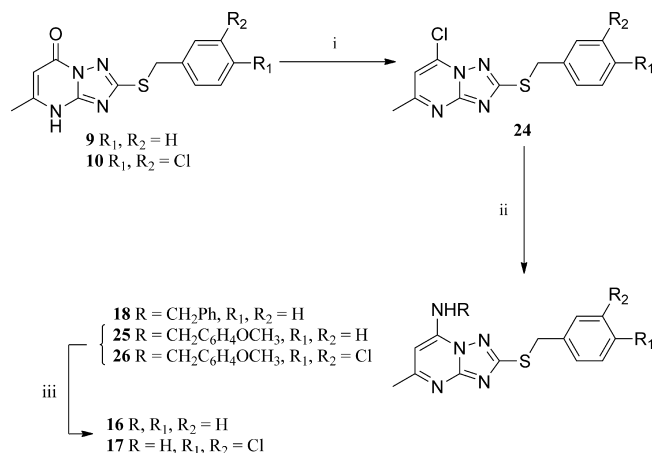
[a](i) PhPOCl₂, 150 °C, 2 h; (ii) NH₂R (1.2 equiv), EtOH, rt, 5 h; (iii) TFA, 85 °C, 25 h (**25** = 29%, **26** = 40%).

Structures of Inhibitors in Complex with *Hs*DHODH. In order to investigate the binding mode of the *S*-benzyltriazolopyrimidines within *Hs*DHODH, compound **12** was cocrystallized with *Hs*DHODH and the resulting structure was solved, using X-ray crystallography, to 1.6 Å resolution. The high quality of the resulting structure is reflected in R_{work} and R_{free} of 16.1% and 17.6%, respectively. As indicated previously, the *Hs*DHODH/compound **12** cocrystal structure was then used to guide the design of compound **15**, for which an additional cocrystal structure with *Hs*DHODH was also obtained with a resolution of 1.55 Å and R_{work}/R_{free} of 15.9%/17.7%, respectively.

Previous structural studies of *Hs*DHODH[21,25] have found that some of the loop regions of the protein were disordered in the crystal structures. This is also true of the structures presented here with respect to the region around residues 69−71, although in contrast to a number of the previously reported structures, in the present case the electron density corresponding to residues 216−225 was readily interpretable in the structures containing both **12** and **15**.

As expected, compounds **12** and **15** both bind within the putative ubiquinone binding channel of *Hs*DHODH, occupying the same pocket that is targeted by previously reported inhibitors. Compounds **12** and **15** both make a pair of key hydrogen bond interactions with the protein, one involving the pyrimidine nitrogen atom of the triazolopyrimidine core and $Y_{Hs}356$ and a second between the carbonyl oxygen of the inhibitors and $Q_{Hs}47$, respectively. These two residues have also been shown to form important polar contacts within other *Hs*DHODH−inhibitor complexes.[26−28] As predicted from our in silico studies, the dichlorobenzyl group of the inhibitors is located within the more hydrophobic part of the binding region, with the closest hydrophobic contacts involving residues $M_{Hs}43$, $L_{Hs}46$, $A_{Hs}59$, $F_{Hs}62$, and $P_{Hs}364$.

The cocrystal structure with **12** showed that the inhibitor fits tightly within the binding cavity. However, a small amount of additional space adjacent to the methyl group at position R_3 (Figure 2) is also apparent, which we reasoned could be exploited in a subsequent design of further inhibitors. Indeed, in light of this observation compound **15**, which has an ethyl group at this position, was designed and synthesized. Interestingly, in vitro enzyme assays revealed that compound
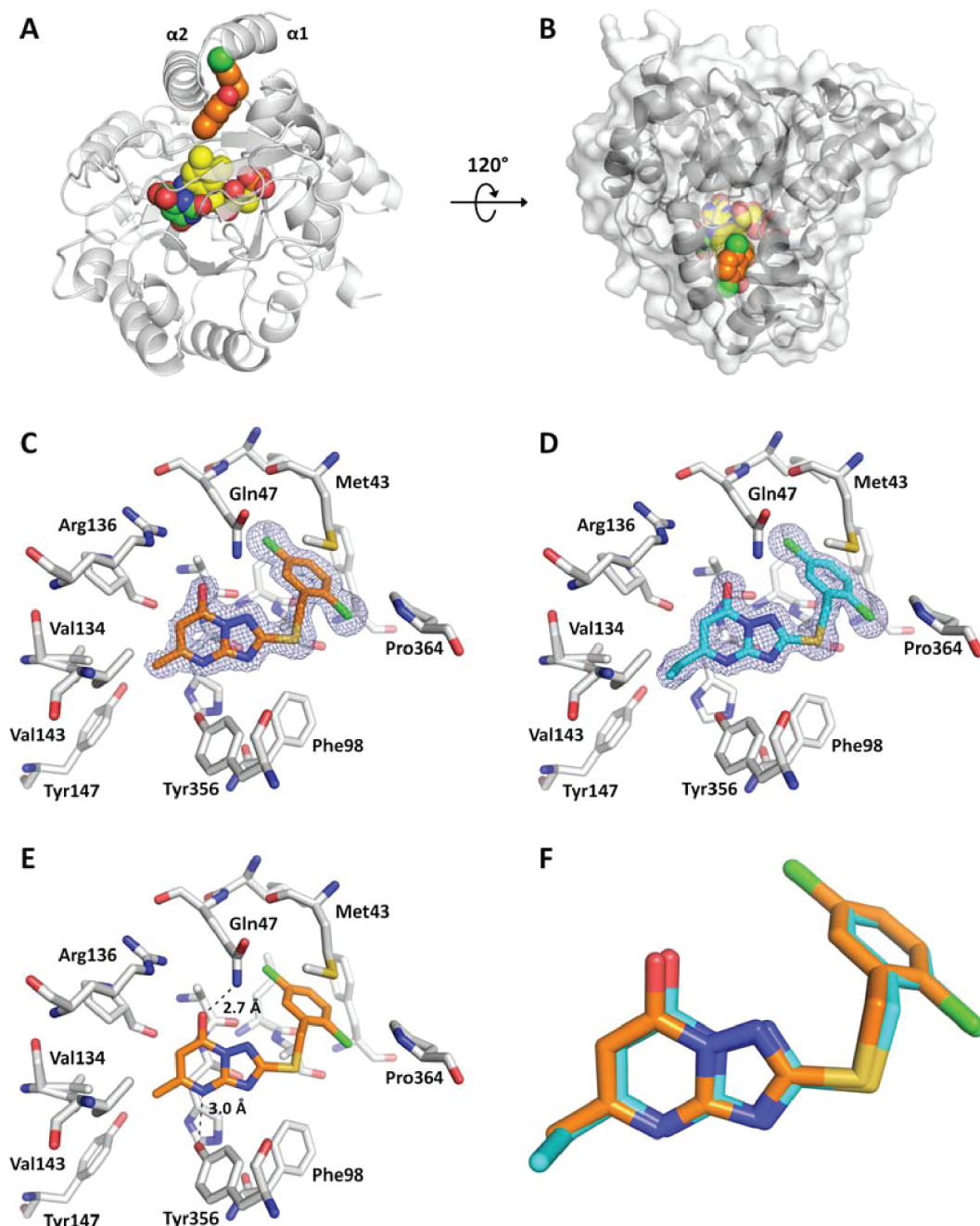
Figure 3. Cocrystal structures of **12** and **15** with *Hs*DHODH. (A) Ribbon diagram of *Hs*DHODH showing the position of compound **12** (carbon atoms shown as orange spheres, other atoms in CPK colors) in the putative ubiquinone binding site, with the cofactor FMN (carbon atoms shown as yellow spheres) and the reaction product orotate (carbon atoms shown as green spheres) at the primary active site of the enzyme. The two helices (α1 and α2) at the N-terminus of the construct that forms the inhibitor binding channel are labeled. (B) Same representation as (A) rotated by 120°, with transparent surface added. (C, D) $2F_o - F_c$ electron density for **12** (carbon atoms in orange) and **15** (carbon atoms in cyan), respectively, contoured at 1.0σ. (E) Hydrogen bonds formed between **12** and *Hs*DHODH. (F) Superimposition of the cocrystal structures of *Hs*DHODH with **12** and **15** (same coloring as for (C) and (D)) shows that the two inhibitors share a near identical binding mode.

15 had a slightly lower IC_{50} when compared to compound **12** against *Hs*DHODH, and the cocrystal structure confirmed that the ethyl group was easily accommodated within the inhibitor binding site. The additional methylene group brings compound **15** to within just 3.6 Å of the FMN cofactor, as well as decreases the distance between the inhibitor and V_{Hs}143 to 4.1 Å (Figure 3).

Novel Binding Modes of Inhibitors within *Hs*DHODH. The molecular viewing program PyMOL[29] was used to align

the cocrystal structures of **12** and **15** (PDB files 3ZWS and 3ZWT, respectively) with all other *Hs*DHODH PDB files available on the Protein Data Bank to date (1D3G, 1D3H, 2B0M, 2BXV, 2FPT, 2FQI, 2FPY, 2PRH, 2PRL, 2PRM, 2WV8, 3FJ6, 3FJL, 3GOU, 3GOX, 3KVJ, 3KVL, 3KVM[21,25−27,30]). The structures aligned well with rms deviations between 0.164 and 0.205 Å. The TIM barrel core and the bound FMN and orotate molecules are all seen to adopt essentially identical poses within the enzyme throughout
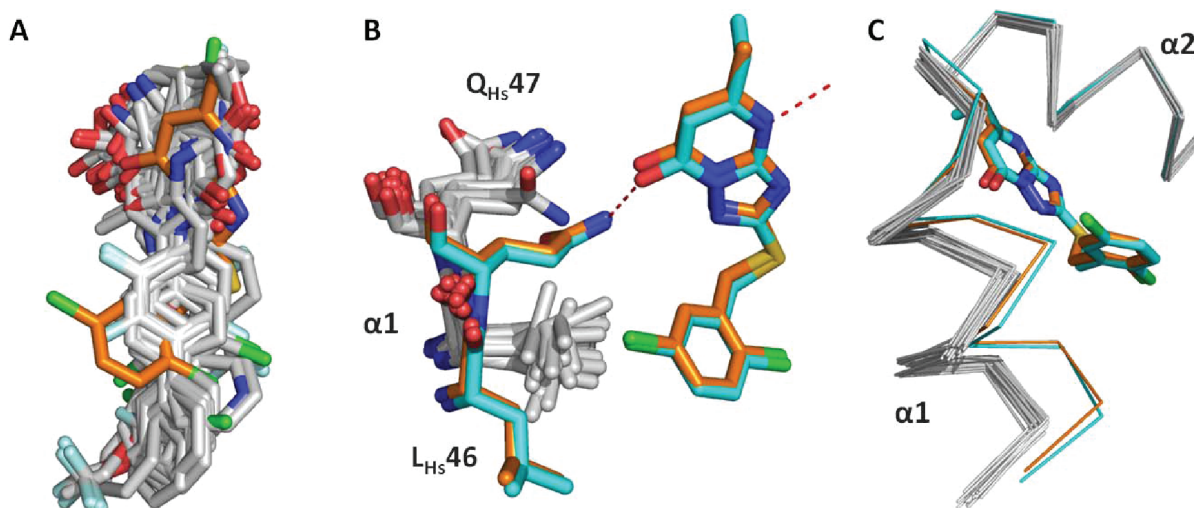
Figure 4. PyMOL[29] alignments of the cocrystal structures of **12** (carbons in orange) and **15** (carbons in cyan) with all other *Hs*DHODH structures in the PDB (carbons in white). (A) Overlay of inhibitors shows that the 2,5-dichlorophenol group of **12** occupies a novel region of space not used by other crystallized inhibitors. (B) The 2,5-dichlorophenyl group in **12** and **15** displaces $L_{Hs}46$ on the $\alpha1$ helix of DHODH. Both $L_{Hs}46$ and $Q_{Hs}47$ undergo displacement, allowing $Q_{Hs}47$ to move close enough to the hydroxyl group of the inhibitors to form a hydrogen bond (red dotted line). (C) The $\alpha1$ helices hinge on the residues at their C-terminus, allowing them to rotate slightly and move by up to 3.1 Å.
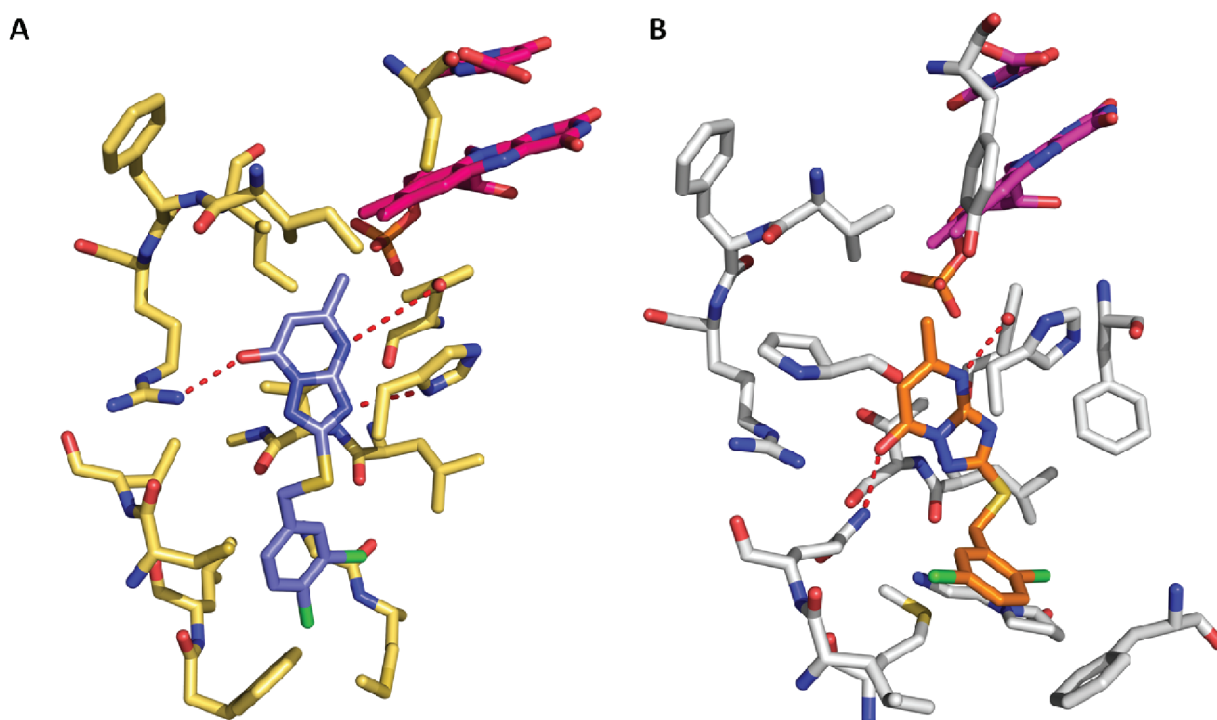

Figure 5. (A) eHiTS[31] docking predictions for compound **10** (carbons in blue) in *Pf*DHODH predicts that the triazolopyrimidine group of the inhibitors occupies a pose very similar to that of **12** (B) (carbons in orange) in *Hs*DHODH. Hydrogen bonds, shown in red, are predicted with $H_{Pf}185$, $Y_{Pf}528$, and $R_{Pf}265$. (B) Crystal structure of compound **12** bound to *Hs*DHODH, in comparison with (A).

these structures. However, comparing the present cocrystal structures to those previously reported reveals substantial differences in the conformation of a helix that forms part of the inhibitor binding site.

Two helices form a "V" shaped lid on the surface of the TIM barrel of type 2 DHODHs. Here, the helices have been termed $\alpha1$ and $\alpha2$, with $\alpha1$ being at the N-terminus (Figure 3A). In all the *Hs*DHODH crystal structures published to date, these "V" helices are in an almost identical "classic" conformation. In contrast, the $\alpha1$ helix in the structures of *Hs*DHODH with **12**

and **15** adopts a slightly rotated conformation up to 3.1 Å away from that seen in all the previous structures (Figure 4).

The adoption of the alternative conformation appears necessary in order to accommodate the 2,5-dichlorobenzyl moiety within compounds **12** and **15**, which would otherwise clash with $L_{Hs}46$ within the $\alpha1$ helix in the classic conformation. This allows $Q_{Hs}47$ to occupy a region where it is close enough to the hydroxyl group within the inhibitors to undergo hydrogen bonding (Figure 4B). It is likely that the size of the 2,5-dichlorobenzyl group in these inhibitors drives this
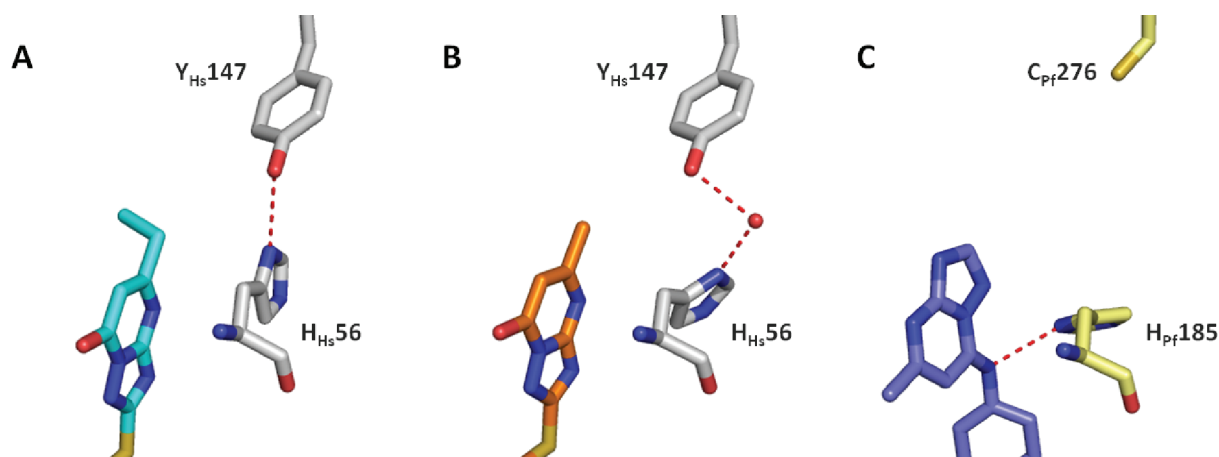
Figure 6. (A) $H_{Hs}56$ forms a direct hydrogen bond to $Y_{Hs}147$ in the *Hs*DHODH structure with compound **15**. (B) $H_{Hs}56$ displays a water-mediated hydrogen bond to $Y_{Hs}147$ in the *Hs*DHODH structure with compound **12**. (C) In *Pf*DHODH $Y_{Hs}147$ is replaced with $C_{Pf}276$, and in all structures to date, the inhibitor is bound to $H_{Pf}185$ with a hydrogen bond. Here, compound **1** bound to *Pf*DHODH is displayed (PDB file 3I65).

displacement. It is interesting that other inhibitors in this series, all of which contain a benzyl group, inhibit *Hs*DHODH substantially less (compounds **1−11**, **13**, **14**, and **16−18**, Table 1). Furthermore, consideration of the gross overall volume occupied by the benzyl portions in these inhibitors broadly corresponds with their observed inhibitory activity. Thus, molecules containing unsubstituted (compound **9**) or 3- or 4-monosubstituted (compounds **2**, **4−7**, and **14**) benzyl groups are relatively compact and show the weakest inhibitory activities. Compounds containing 2-monosubstituted benzyl systems (compounds **3** and **8**) and dihalo-substituted benzyl moieties (compounds **10−12** and **15**) generally show improved inhibitory activity.

The sizable conformational change in the inhibitor binding pocket is likely to be a major contributing factor to the observed switch in selectivity of this series from *Pf*DHODH to *Hs*DHODH. The α1 helix in the cocrystal structures of **12** and **15** is in a different conformation relative to the rest of the protein when compared to 18 other *Hs*DHODH structures, including a proposed apo structure.[27] This suggests that the alternative conformation is stabilized by inhibitor binding.

Predicted Binding Mode of Inhibitors in *Pf*DHODH. In order to compare and contrast the binding modes of the inhibitors with the human and *P. falciparum* enzymes, the docking software eHiTS[31] was used in conjunction with the reported *Pf*DHODH crystal structure (PDB code 1TV5) to predict the binding mode of the most active *Pf*DHODH inhibitors, compounds **2** and **10**, within the known inhibitor binding site. eHiTS treats the receptor as a rigid structure and divides the ligands into rigid fragments and flexible connecting chains. For eHiTS, the "clip" or the active site was defined as the cavity containing the inhibitor bound in the crystal structure, and the receptor was defined as a 10 Å cut from the edges of this clip region. Additionally, a setting of "maximum" was used for the accuracy variable within these docking runs.

Inspection of the resulting predicted binding poses reveals that most of the low energy poses are very similar to those found in the X-ray structures of the same ligands within *Hs*DHODH (Figure 5). This predicted binding mode is consistent with the observed lack of activity of compounds **14−18** in the presence of PfDHODH (Table 1). In this pose, replacement of the acceptor oxygen in the active compounds (**9**

and **10**) by donor hydrogen bond (**16−18**) amino groups creates an extremely unfavorable interaction with Arg265. Equally, replacement of the methyl group of the active compounds (**2** and **12**) with the bulkier ethyl group (compounds **14** and **15**) causes an unfavorable steric clash between the ligands and the protein.

Site Directed Mutagenesis of *Hs*DHODH and *Pf*DHODH. The *Hs*DHODH cocrystal structures with compounds **12** and **15** align very well with each other. Indeed, all but one of the side chains from residues that line the binding site occupy almost identical conformations. The variant residue is $H_{Hs}56$, which in the structure with compound **15** appears to form a direct hydrogen bond with residue $Y_{Hs}147$. However, with compound **12**, the equivalent bond appears to be water-mediated. Consequently, in the cocrystal structure with compound **15**, $H_{Hs}56$ is located slightly further into the inhibitor binding site (Figure 6). These two different conformations for $H_{Hs}56$ are seen in almost a 50:50 ratio throughout the *Hs*DHODH structures in the PDB, and structure 2WV8 is depicted as having a share of both. This and the fact that the structures with compounds **12** and **15** are otherwise extremely similar suggest that the energy difference between the two conformations of this histidine is low and that $H_{Hs}56$ may be able to interchange between them depending on the binding of a specific inhibitor.

In order to probe the role of this histidine in terms of the efficiency of inhibition for the present inhibitors, mutations of the $H_{Hs}56$ and $Y_{Hs}147$ residues were carried out and the resulting enzymes were tested against key compounds from the *S*-benzyltriazolopyrimidine series (Table 2). The reduced affinity of the compounds to the $H_{Hs}56A$ mutant supports

Table 2. Fold Change in IC$_{50}$ in *Hs*DHODH Mutants ((Mutant IC$_{50}$)/(*Hs*DHODH IC$_{50}$))[a]

compd	*Hs*DHODH	$H_{Hs}56A$	$Y_{Hs}147A$	$Y_{Hs}147C$	$Y_{Hs}147F$
2	1	nsi	nsi	nsi	nsi
10	1	nsi	nsi	nsi	8.8
12	1	7.1	20	14	1.1
15	1	17	16	9	1.9

[a]nsi: no significant inhibition (<50% at 100 μM inhibitor concentration).

the hypothesis that $H_{Hs}56$ is important for inhibitor binding. Removing this residue causes a loss of detectable binding for compounds **2** and **10** and a large reduction in binding of **12** and **15**. Compounds **12** and **15** show a decreased affinity to the $Y_{Hs}147A$ and $Y_{Hs}147C$ mutants but do not display a significant change in binding with the $Y_{Hs}147F$ mutant. This is in contrast to the behavior of compounds **2** and **10** which display a significant loss of binding against all mutants, suggesting a difference in binding mode between the more active **12** and **15** and the less active **2** and **10**.

In contrast to observations of the contacts between inhibitors with $H_{Hs}56$ in the majority of the reported *Hs*DHODH structures, the docking of compounds **2** and **10** into *Pf*DHODH suggests that the pyrimidine NH group of the inhibitors forms a direct hydrogen bond with the analogous $H_{Pf}185$ residue (Figure 6C). Indeed, this prediction is supported by the fact that a hydrogen bond between the bound inhibitor and $H_{Pf}185$ is observed in all the *Pf*DHODH crystal structures to date.[18,32,33]

The equivalent residue to $Y_{Hs}147$, $C_{Pf}276$, cannot form a polar contact with the $H_{Pf}185$ in *Pf*DHODH. This allows $H_{Pf}185$ to display its polar nitrogen to the inhibitor binding pocket. We have previously suggested that this conformational difference between $H_{Hs}56$ and $H_{Pf}185$ is a key contributor to selectivity.[7] Mutations of $H_{Pf}185$ and $C_{Pf}276$ were carried out and tested against key compounds from the *S*-benzyltriazolopyrimidine series (Table 3).

Table 3. Fold Change in IC_{50} in *Pf*DHODH Mutants $((\text{Mutant } IC_{50})/(Pf\text{DHODH } IC_{50}))$[a]

compd	*Pf*DHODH	$H_{Pf}185A$	$C_{Pf}276A$	$C_{Pf}276F$	$C_{Pf}276Y$	$F_{Pf}188A$
1	1	19	0.69	2.3	3.5	29
2	1	nsi	1.5	nsi	nsi	nsi
10	1	nsi	2.0	nsi	nsi	nsi
12	1	nsi	3.7	nsi	nsi	nsi
15	nsi	nsi	nsi	nsi	nsi	nsi

[a]nsi: no significant inhibition (<50% at 100 μM inhibitor concentration).

As with the $H_{Hs}56$ in *Hs*DHODH, the docking predictions indicate that the inhibitors show a dependence on $H_{Pf}185$ for binding in *Pf*DHODH. Indeed, replacing this residue with alanine ($H_{Pf}185A$) causes a complete loss of inhibition with compounds **2**, **10**, **12**, and **15** and a substantial loss of inhibition with the previously published inhibitor **1**. Replacing $C_{Pf}276$ with a similar-sized alanine residue causes only minor changes in inhibition, but replacement with a much larger phenylalanine or tyrosine residue (mutation $C_{Pf}276F$ or $C_{Pf}276Y$, respectively) causes loss of inhibition for all compounds in this series.

The $F_{Pf}188A$ mutant caused a large loss of *Pf*DHODH inhibition with all the compounds, showing that for the *S*-benzyltriazolopyrimidines (and compound **1**) this residue is very important for binding. This has also been previously shown with other inhibitors of *Pf*DHODH.[33]

■ DISCUSSION

Two compounds in the series (**12** and **15**) displayed potent activity against *Hs*DHODH (Table 1). This inhibitory activity is comparable to other potent inhibitors of *Hs*DHODH including A77 1726, the active metabolite of leflunomide, a drug currently used to treat rheumatoid arthritis.[34]

Compounds **12** and **15** have IC_{50} values over 10 000 times lower against *Hs*DHODH than those found for the other compounds in the series. This significant difference appears to result from the introduction of a chlorine substituent at the 2-position of the benzyl group of the inhibitors. The cocrystal structures of these compounds in *Hs*DHODH were obtained and compared to previously reported *Hs*DHODH and *Pf*DHODH structures, which revealed that the current structures display a number of interesting and novel features including a large movement in the α1 helix at the N-terminal of the *Hs*DHODH enzyme. The α1 helix slightly rotates and moves relative to its position in the reported structures, by over 3 Å. This novel conformational shift appears to be driven by the presence of the inhibitors (Figures 4 and 7). The compounds that induce this structural shift have a bulky 2,5-dichlorobenzyl group which is seen to fill an area of space occupied by $L_{Hs}46$ in all other *Hs*DHODH structures. This causes $L_{Hs}46$ to be displaced and stabilizes the α1 helix in this novel conformation which allows $Q_{Hs}47$ to form an H-bond to the hydroxyl (or carbonyl) group of the inhibitor. It is likely that the other
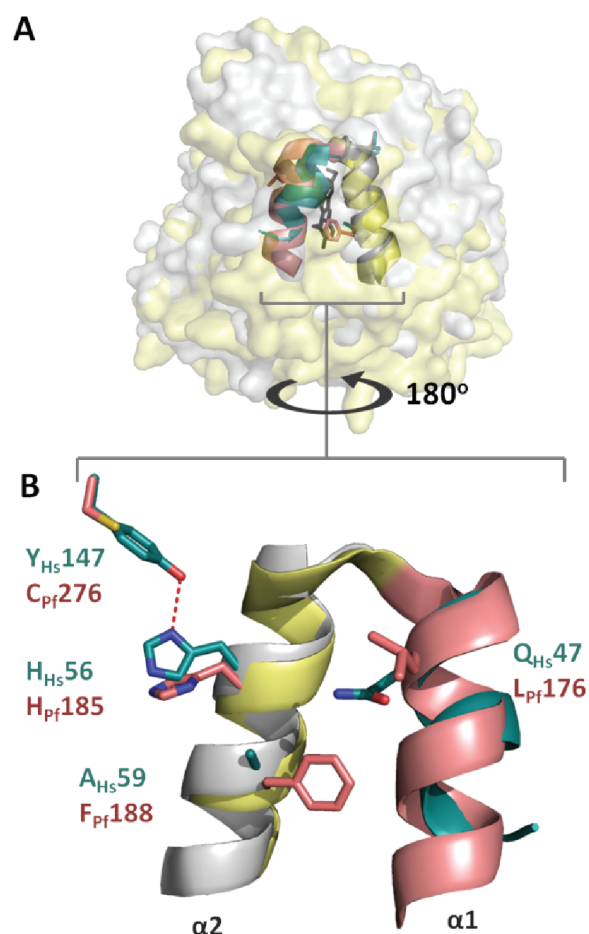

Figure 7. Elements of the inhibitor binding site important for selective binding. (A) PyMOL structural alignment of *Pf*DHODH (colored gold, from structure 1TV5) with *Hs*DHODH with **12** (colored gray, from structure 3ZWS). The N-terminal "V" helices (termed α1 and α2) that form the lid of the binding pocket are shown as cartoons. Elements determined as important for selectivity, including the N-terminal α helix, are colored red in *Pf*DHODH and green in *Hs*DHODH. Compound **12** is shown in the inhibitor binding site in black. (B) Shown are the V helices from the protein interior. Key residues involved in selective binding are labeled.

compounds in this series do not cause this change in conformation, as they lack a substituent in the 2-position of the benzyl group.

In crystal structures of *Pf*DHODH the analogous α1 helix has also been observed in two conformations.[33] However, the sequence and structural differences between the two orthologues at this position are substantial, suggesting that differences in inhibitor structure that cause a conformational change to the α1 helix in one enzyme may have not have the same effect in the analogous enzyme from a different organism. Indeed, the differences in sequence and structure of the N-terminal helices accompanied by their apparent flexibility and ability to adopt differing conformations are likely to be very important in inhibitor selectivity.

Recently, electron spin resonance was used to detect a significant amount of flexibility in the α1 helix of *E. coli* DHODH.[35] This along with conformational variation of the homologous helices seen in X-ray crystal structures of rat,[36] *P. falciparum*,[33] and now human DHODHs suggests that movement and flexibility of this helix may be common across family 2 DHODHs. It is possible that the flexibility of this helix is important for the substrate (CoQ) to gain access to the active site and that stabilizing the helix in an unfavorable conformation could be a mechanism by which small molecule binding induces inhibition.

Docking of the described compounds in *Pf*DHODH using eHiTS suggests a binding mode similar to that observed within the *Hs*DHODH structures. This allows a hydrogen bond to be formed with $H_{Pf}185$, a residue that is seen bound to the inhibitors in all *Pf*DHODH cocrystal structures to date.[18,32,33]

Two different conformations of $H_{Hs}56$ are seen throughout all the crystal structures of *Hs*DHODH. One conformation shows direct hydrogen bonding to $Y_{Hs}147$, while the other shows the bond to be water-mediated, allowing $H_{Hs}56$ to move closer to the inhibitor. The fact that cocrystal structures with **12** and **15** are so similar, but $H_{Hs}56$ is seen populating a different conformation in both, suggests that there is only a small energy difference between the two states.

The $Y_{Hs}147F$ mutant cannot form a hydrogen bond with $H_{Hs}56$ either directly or via water molecules. This mutation has very little effect on the binding of **12** and **15**, suggesting that an interaction between $H_{Hs}56$ and $Y_{Hs}147$ is not essential in the novel binding mode displayed by these compounds. However, the presence of $H_{Hs}56$ does seem to be important as demonstrated by the $H_{Hs}56A$ mutant, but it is likely to be able to move between the two conformations, seen in the crystal structures, relatively freely. The binding of the other inhibitors in the series is more substantially affected by the $Y_{Hs}147F$ mutation, supporting the idea that they bind to the enzyme in a different pose to the more active **12** and **15**.

The observed conformation of $H_{Hs}56$ in HsDHODH is in contrast to the conformation found for the analogous $H_{Pf}185$ residue in *Pf*DHODH. This is likely to be due to the lack of a tyrosine residue in the position corresponding to $Y_{Hs}147$ in *Pf*DHODH. Here, the tyrosine is replaced with a cysteine, $C_{Pf}276$, whose side chain cannot form an intramolecular H-bond with the histidine. This allows the histidine to rotate and display its δ nitrogen atom to the inhibitor binding site (Figure 7). The docking predictions and observations derived from inspection of the crystal structures suggest that $H_{Pf}185$ forms a hydrogen bond with inhibitors. The change in the hydrogen bonding behavior in this region of the binding site resulting from the conformational differences in this histidine is likely to

be a key contributor to the observed selectivity between the human and plasmodial enzymes.

The mutations of $Y_{Hs}147$ and $C_{Pf}276$ show that the size of a residue at this position is important for inhibitor binding as well as its hydrogen bonding potential. In *Pf*DHODH smaller cysteine and alanine residues allow better inhibitor binding, but in *Hs*DHODH the larger phenylalanine and tyrosine residues are favored. The sizes of the residues at this position are likely to affect inhibitor binding by altering the positions of $H_{Pf}185$ and $H_{Hs}56$ in the respective enzymes. This is because they only contact the residue indirectly, through H-bonding mediated via the histidine.

Other key contributions to specificity in the enzymes are provided by $Q_{Hs}47$ in *Hs*DHODH and $F_{Pf}188$ in *Pf*DHODH. Residue $Q_{Hs}47$, which can be seen hydrogen-bonding to the inhibitors in the *Hs*DHODH structures presented here, is not present at the corresponding position in *Pf*DHODH, implying that alternative interactions need to be utilized for binding of inhibitors to this enzyme.

Mutations of $F_{Pf}188$ show that this residue is essential for the binding of the inhibitors presented here to *Pf*DHODH, as well as previously published compounds.[33] This is likely to be due to the ability of this residue to provide π stacking interactions with aromatic moieties present within the inhibitor. In *Hs*DHODH, this residue is replaced by an alanine ($A_{Hs}59$), which cannot contribute to binding in the same way, implying that potent inhibitors of this enzyme must acquire binding affinity through alternative interactions.

■ CONCLUSIONS

In order to explore the factors dictating the selectivity of inhibitor binding to both human and plasmodial DHODH, the in silico molecular similarity matching program ROCS was applied to a library derived from the Maybridge chemical screening collection in order to identify a novel DHODH inhibitor template. Analogous compounds were synthesized using information from crystallography and docking studies, and it was found that minor differences in compound structure resulted in major differences in inhibitor affinity and in some cases in dramatic switches in specificity between *Pf*DHODH and *Hs*DHODH.

Crystal structures of the inhibitors in *Hs*DHODH revealed a structural change in the N-terminal helix that has not been reported in any other *Hs*DHODH crystal structure. This relative "movement" seems to be driven by the shape of the bound inhibitor and is accompanied by a substantial increase in inhibitory activity. Although a similar movement has been described in the analogous helix of *Pf*DHODH,[33] the structural differences between the human and plasmodial enzymes in this region suggest that the induced changes in *Hs*DHODH would not be replicated in *Pf*DHODH with these compounds. Therefore, the structural plasticity in these regions not only allows binding of a variety of different chemical scaffolds but is a key factor that allows specific binding of inhibitors to both enzymes.

The equivalent $H_{Hs}56$ and $H_{Pf}185$ residues also vary in conformation. Residue $H_{Hs}56$ displays modest changes in position and hydrogen bonding networks between *Hs*DHODH structures containing different classes of inhibitors, and $H_{Pf}185$ adopts an altogether different pose in *Pf*DHODH that allows hydrogen bonding with inhibitors. The flexibility in position and orientation of the side chain of this residue appears to contribute to the observation that differing inhibitor scaffolds

can be readily accommodated in both *Pf*DHODH and *Hs*DHODH, and the larger observed difference in conformation and subsequently hydrogen bonding potential contributes to the specificity of inhibitor binding between the enzymes.

We have synthesized a series of novel inhibitors with a unique binding mode in *Hs*DHODH that could be exploited in the development of treatments of rheumatoid arthritis, multiple sclerosis,[3] cancer,[4] and viral infections.[5,6] Additionally, a library of analogues has allowed us to identify key features of *Pf*DHODH and *Hs*DHODH that are important in governing the specificity of inhibitor binding between the enzymes. This information can be used to aid the synthesis of further compounds with selective activity against *Pf*DHODH without inhibiting *Hs*DHODH, a prerequisite of any *Pf*DHODH inhibitor that can be considered for the treatment of malaria.

■ ASSOCIATED CONTENT

Ⓢ Supporting Information

Structures of commercial compounds purchased as a result of the in silico screen, kinetic characterization of mutants, and additional information on crystallography, biological techniques, and experimental data. This material is available free of charge via the Internet at http://pubs.acs.org.

Accession Codes

The PDB codes for structures **12** and **15** are 3ZWS and 3ZWT, respectively.

■ AUTHOR INFORMATION

Corresponding Author

*For G.A.M.: phone, +44 113 3432908; fax, +44 113 3432835; e-mail, g.a.mcconkey@leeds.ac.uk. For C.W.G.F.: phone, +44 113 3436510; fax, +44 113 3436565; e-mail, c.w.g.fishwick@leeds.ac.uk. For A.P.J.: phone, +44 113 3436515; fax, +44 113 3436565; e-mail, a.p.johnson@leeds.ac.uk.

Notes

The authors declare no competing financial interest.

■ ABBREVIATIONS USED

*Hs*DHODH, *Homo sapiens* dihydroorotate dehydrogenase; *Pf*DHODH, *Plasmodium falciparum* dihydroorotate dehydrogenase; ROCS, rapid overlay of chemical structures; TIM, triosephosphate isomerase barrel structural motif

■ REFERENCES

(1) McRobert, L.; McConkey, G. A. RNA interference (RNAi) inhibits growth of *Plasmodium falciparum*. *Mol. Biochem. Parasitol.* **2002**, *119*, 273–278.

(2) Breedveld, F. C.; Dayer, J. M. Leflunomide: mode of action in the treatment of rheumatoid arthritis. *Ann. Rheum. Dis.* **2000**, *59*, 841–849.

(3) Palmer, A. M. Teriflunomide, an inhibitor of dihydroorotate dehydrogenase for the potential oral treatment of multiple sclerosis. *Curr. Opin. Invest. Drugs* **2010**, *11*, 1313–1323.

(4) Chen, S.-F.; Ruben, R.; Dexter, D. Mechanism of action of the novel anticancer agent 6-fluoro-2-(2′-fluoro-1,1′-biphenyl-4-yl)-3-methyl-4-quinolinecarboxylic acid sodium salt (NSC 368390): inhibition of de novo pyrimidine nucleotide biosynthesis. *Cancer Res.* **1986**, *46*, 5014–5019.

(5) Hoffmann, H.; Kunz, A.; Simon, V. A.; Palese, P.; Shaw, M. L. Broad-spectrum antiviral that interferes with de novo pyrimidine biosynthesis. *Proc. Natl. Acad. Sci. U.S.A.* **2011**, *108*, 5777–5782.

(6) Qing, M.; Zou, G.; Wang, Q.-Y.; Xu, H. Y.; Dong, H.; Yuan, Z.; Shi, P.-Y. Characterization of dengue virus resistance to brequinar in cell culture. *Antimicrob. Agents Chemother.* **2010**, *54*, 3686–3695.

(7) Cowen, D.; Bedingfield, P.; McConkey, G. A.; Fishwick, C. W. G.; Johnson, A. P. A study of the effects of substituents on the selectivity of the binding of *N*-arylaminomethylene malonate inhibitors to DHODH. *Bioorg. Med. Chem. Lett.* **2010**, *20*, 1284–1287.

(8) Phillips, M. A.; Rathod, P. K. Plasmodium dihydroorotate dehydrogenase: a promising target for novel anti-malarial chemotherapy. *Infect. Disord. Drug Targets* **2010**, *10*, 226–239.

(9) Fritzson, I.; Bedingfield, P. T. P.; Sundin, A. P.; McConkey, G.; Nilsson, U. J. N-Substituted salicylamides as selective malaria parasite dihydroorotate dehydrogenase inhibitors. *MedChemComm* **2011**, *2*, 895–898.

(10) Murray, C. J.; Rosenfeld, L. C.; Lim, S. S.; Andrews, K. G.; Foreman, K. J.; Haring, D.; Fullman, N.; Naghavi, M.; Lozano, R.; Lopez, A. D. Global malaria mortality between 1980 and 2010: a systematic analysis. *Lancet* **2012**, *379*, 413–431.

(11) Booker, M. L.; Bastos, C. M.; Kramer, M. L.; Barker, R. H.; Skerlj, R.; Bir Sidhu, A.; Deng, X.; Celatka, C.; Cortese, J. F.; Guerrero Bravo, J. E.; Krespo Llado, K. N.; Serrano, A. E.; Angulo-Barturen, I.; Jimenez-Diaz, M. B.; Viera, S.; Garuti, H.; Wittlin, S.; Papastogiannidis, P.; Lin, J.-W.; Janse, C. J.; Khan, S. M.; Duraisingh, M.; Coleman, B.; Goldsmith, E. J.; Phillips, M. a; Munoz, B.; Wirth, D. F.; Klinger, J. D.; Wiegand, R.; Sybertz, E. Novel inhibitors of *Plasmodium falciparum* dihydroorotate dehydrogenase with anti-malarial activity in the mouse model. *J. Biol. Chem.* **2010**, *285*, 33054–33064.

(12) Phillips, M. A.; Rathod, P. K.; Gujjar, R.; Marwaha, A. S.; Charman, S. A. Dihydroorotate Dehydrogenase Inhibitors with Selecetive Anti-Malarial Activity. International Patent WO/2009/082691 A1, 2009.

(13) Boa, A. N.; Canavan, S. P.; Hirst, P. R.; Ramsey, C.; McConkey, G. A.; Stead, A. M. W. Synthesis of brequinar analogue inhibitors of malaria parasite dihydroorotate dehydrogenase. *Bioorg. Med. Chem.* **2005**, *13*, 1945–1967.

(14) Heikkilä, T.; Ramsey, C.; Davies, M.; Galtier, C.; Stead, A. M. W.; Johnson, A. P.; Fishwick, C. W. G.; Boa, A. N.; McConkey, G. A. Design and synthesis of potent inhibitors of the malaria parasite dihydroorotate dehydrogenase. *J. Med. Chem.* **2007**, *50*, 186–191.

(15) Heikkilä, T.; McConkey, A. G.; Thirumalairajan, S.; Davies, M.; Parsons, M. R.; McConkey, G. A.; Fishwick, C. W. G.; Johnson, A. P. The first de novo designed inhibitors of *Plasmodium falciparum* dihydroorotate dehydrogenase. *Bioorg. Med. Chem. Lett.* **2006**, *16*, 88–92.

(16) Phillips, M. A.; Malmquist, N. A.; Gujjar, R.; White, J.; El Mazouni, F.; Baldwin, J.; Rathod, P. K. Triazolopyrimidine-based dihydroorotate dehydrogenase inhibitors with potent and selective activity against the malaria parasite *Plasmodium falciparum*. *J. Med. Chem.* **2008**, *51*, 3649–3653.

(17) Gujjar, R.; Marwaha, A.; El Mazouni, F.; White, J.; White, K. L.; Creason, S.; Shackleford, D. M.; Baldwin, J.; Charman, W. N.; Buckner, F. S.; Charman, S.; Rathod, P. K.; Phillips, M. A. Identification of a metabolically stable triazolopyrimidine-based dihydroorotate dehydrogenase inhibitor with antimalarial activity in mice. *J. Med. Chem.* **2009**, *52*, 1864–1872.

(18) Gujjar, R.; El Mazouni, F.; White, K. L.; White, J.; Creason, S.; Shackleford, D. M.; Deng, X.; Charman, W. N.; Bathurst, I.; Burrows, J.; Floyd, D. M.; Matthews, D.; Buckner, F. S.; Charman, S. A.; Phillips, M. A.; Rathod, P. K. Lead-optimization of aryl and aralkyl amine based triazolopyrimidine inhibitors of *Plasmodium falciparum* dihydroorotate dehydrogenase with anti-malarial activity in mice. *J. Med. Chem.* **2011**, *54*, 3935–3949.

(19) Hawkins, P. C. D.; Skillman, A. G.; Nicholls, A. Comparison of shape-matching and docking as virtual screening tools. *J. Med. Chem.* **2007**, *50*, 74–82.

(20) Boström, J.; Greenwood, J. R.; Gottfries, J. Assessing the performance of OMEGA with respect to retrieving bioactive conformations. *J. Mol. Graphics Modell.* **2003**, *21*, 449−462.

(21) Davies, M.; Heikkilä, T.; McConkey, G. A.; Fishwick, C. W. G.; Parsons, M. R.; Johnson, A. P. Structure-based design, synthesis, and characterization of inhibitors of human and *Plasmodium falciparum* dihydroorotate dehydrogenases. *J. Med. Chem.* **2009**, *52*, 2683−2693.

(22) Revankar, G. R.; Robins, R. K. Synthesis and biological activity of some nucleosides resembling guanosine: imidazo[1,2-*a*]pyrimidine nucleosides. *Ann. N.Y. Acad. Sci.* **1975**, *255*, 166−176.

(23) Reiter, J. On triazoles. XXXIX . Synthesis and structure of some 1,2,4-triazolo[1,5-*a*]pyrimidin-5-one oximes. *J. Heterocycl. Chem.* **1997**, *34*, 1519−1526.

(24) Novinson, T.; Springer, R.; O'Brien, D. E.; Scholten, M. B.; Miller, J. P.; Robins, R. K. 2-(Alkylthio)-1,2,4-triazolo[1,5-*a*]-pyrimidines as adenosine 3′,5′-monophosphate phosphodiesterase inhibitors with potential as new cardiovascular agents. *J. Med. Chem.* **1982**, *25*, 420−426.

(25) Liu, S.; Neidhardt, E. A.; Grossman, T. H.; Ocain, T.; Clardy, J. Structures of human dihydroorotate dehydrogenase in complex with antiproliferative agents. *Structure* **2000**, *8*, 25−33.

(26) Hurt, D. E.; Sutton, A. E.; Clardy, J. Brequinar derivatives and species-specific drug design for dihydroorotate dehydrogenase. *Bioorg. Med. Chem. Lett.* **2006**, *16*, 1610−1615.

(27) Walse, B.; Dufe, V. T.; Svensson, B.; Fritzson, I.; Dahlberg, L.; Khairoullina, A.; Wellmar, U.; Al-Karadaghi, S. The structures of human dihydroorotate dehydrogenase with and without inhibitor reveal conformational flexibility in the inhibitor and substrate binding sites. *Biochemistry* **2008**, *47*, 8929−8936.

(28) Baumgartner, R.; Walloschek, M.; Kralik, M.; Gotschlich, A.; Tasler, S.; Mies, J.; Leban, J. Dual binding mode of a novel series of DHODH inhibitors. *J. Med. Chem.* **2006**, *49*, 1239−1247.

(29) *The PyMOL Molecular Graphics System*, version 1.3r1; Schrödinger, LLC: New York, 2010.

(30) McLean, L. R.; Zhang, Y.; Degnen, W.; Peppard, J.; Cabel, D.; Zou, C.; Tsay, J. T.; Subramaniam, A.; Vaz, R. J.; Li, Y. Discovery of novel inhibitors for DHODH via virtual screening and X-ray crystallographic structures. *Bioorg. Med. Chem. Lett.* **2010**, *20*, 1981−1984.

(31) Zsoldos, Z.; Reid, D.; Simon, A.; Sadjad, B. S.; Johnson, A. P. eHiTS: an innovative approach to the docking and scoring function problems. *Curr. Protein Pept. Sci.* **2006**, *7*, 421−435.

(32) Hurt, D. E.; Widom, J.; Clardy, J. Structure of *Plasmodium falciparum* dihydroorotate dehydrogenase with a bound inhibitor. *Acta Crystallogr., Sect. D: Biol. Crystallogr.* **2006**, *62*, 312−323.

(33) Deng, X.; Gujjar, R.; El Mazouni, F.; Kaminsky, W.; Malmquist, N. A.; Goldsmith, E. J.; Rathod, P. K.; Phillips, M. A.; Mazouni, F. E.; Health, G.; France, P. Structural plasticity of malaria dihydroorotate dehydrogenase allows selective binding of diverse chemical scaffolds. *J. Biol. Chem.* **2009**, *284*, 26999−27009.

(34) Herrmann, M. L.; Schleyerbach, R.; Kirschbaum, B. J. Leflunomide: an immunomodulatory drug for the treatment of rheumatoid arthritis and other autoimmune diseases. *Immunopharmacology* **2000**, *47*, 273−289.

(35) Couto, S. G.; Cristina Nonato, M.; Costa-Filho, A. J. Site directed spin labeling studies of *Escherichia coli* dihydroorotate dehydrogenase N-terminal extension. *Biochem. Biophys. Res. Commun.* **2011**, *414*, 487−492.

(36) Hansen, M.; LeNours, J.; Johansson, E.; Antal, T.; Ullrich, A.; Loffler, M.; Larsen, S. Inhibitor binding in a class 2 dihydroorotate dehydrogenase causes variations in the membrane-associated N-terminal domain. *Protein Sci.* **2004**, *13*, 1031−1042.